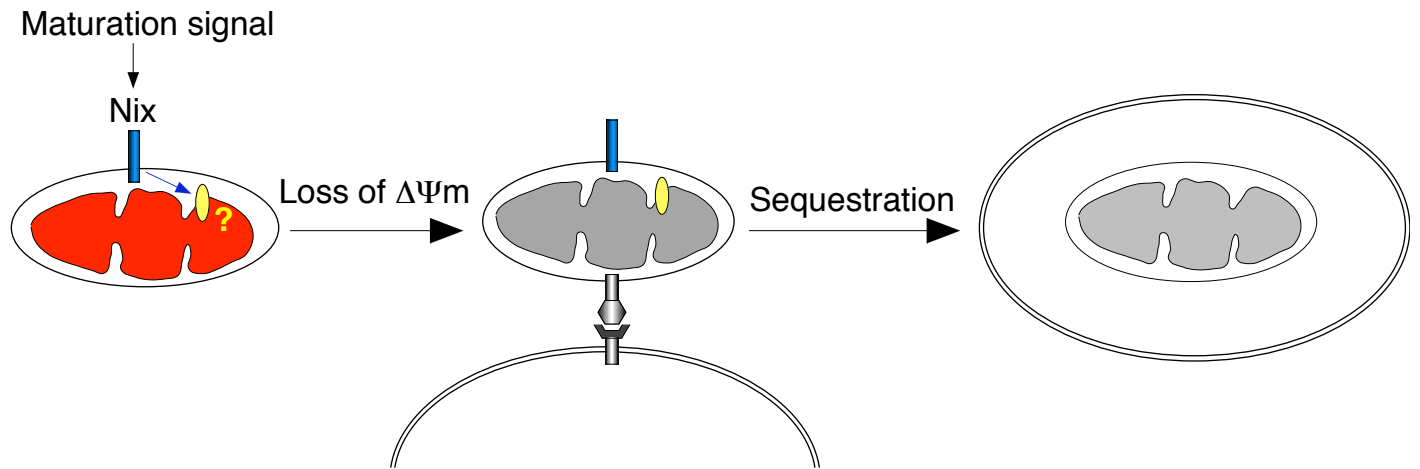
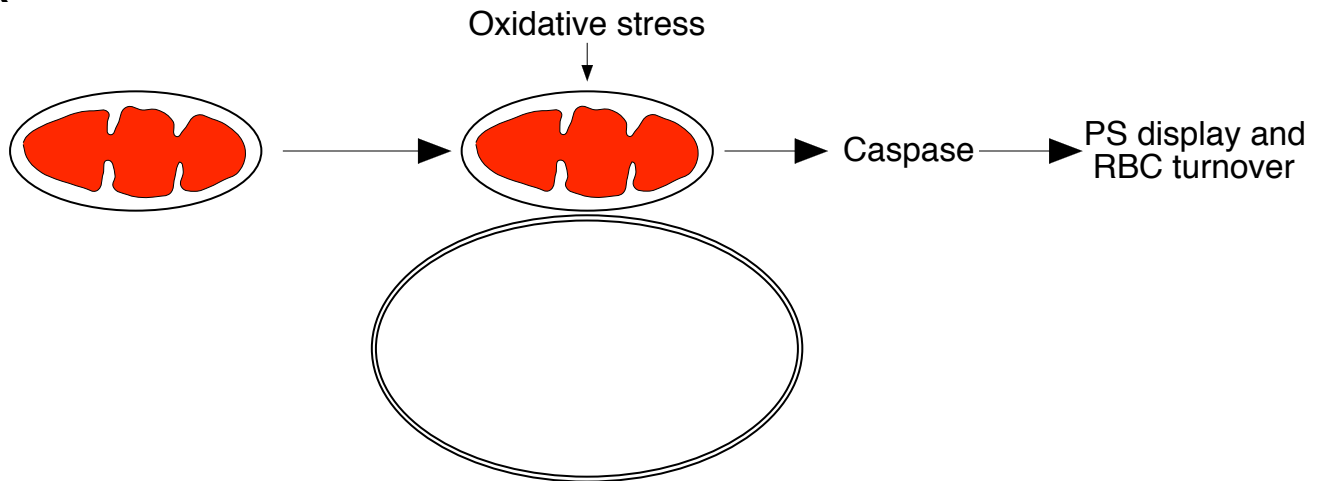


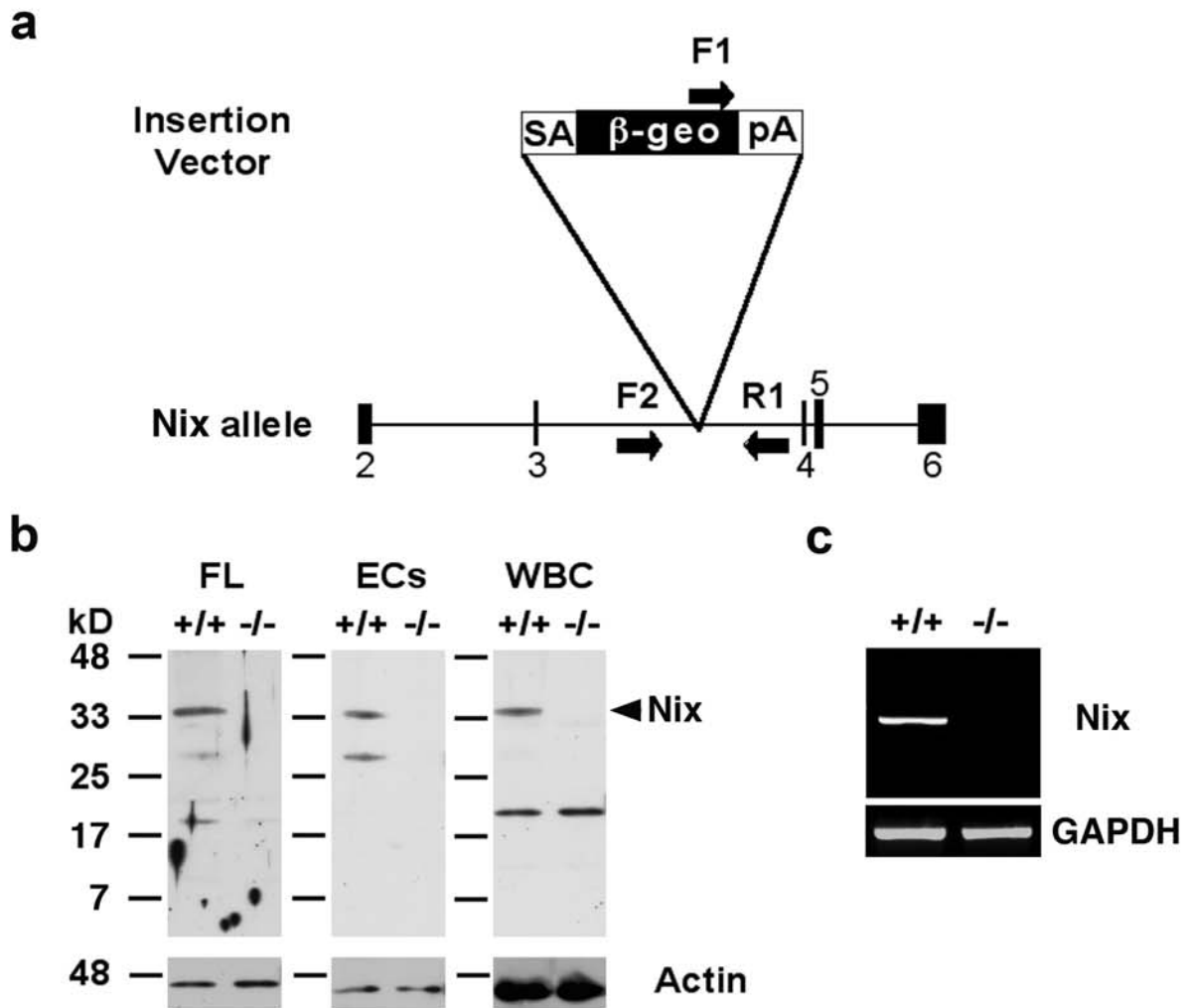
Supplementary Table 1. Whole Blood cell analysis of Nix^{-/-} mice

	WT (n=11)	Nix ^{-/-} (n=11)	P value
WBC (10 ³ /uL)	8 ± 0.6	9.7 ± 1.5	0.29
RBC (10 ⁶ /uL)	11.1 ± 0.1	8.9 ± 0.4	<0.0001
HB (g/dL)	16.7 ± 0.3	15.2 ± 0.5	0.02
HCT (%)	52.6 ± 0.5	47.4 ± 1.7	0.008
MCV (fL)	47.3 ± 0.3	53.5 ± 1	<0.0001
Platelets (10 ³ /uL)	1057 ± 87.7	1308 ± 62.9	0.03

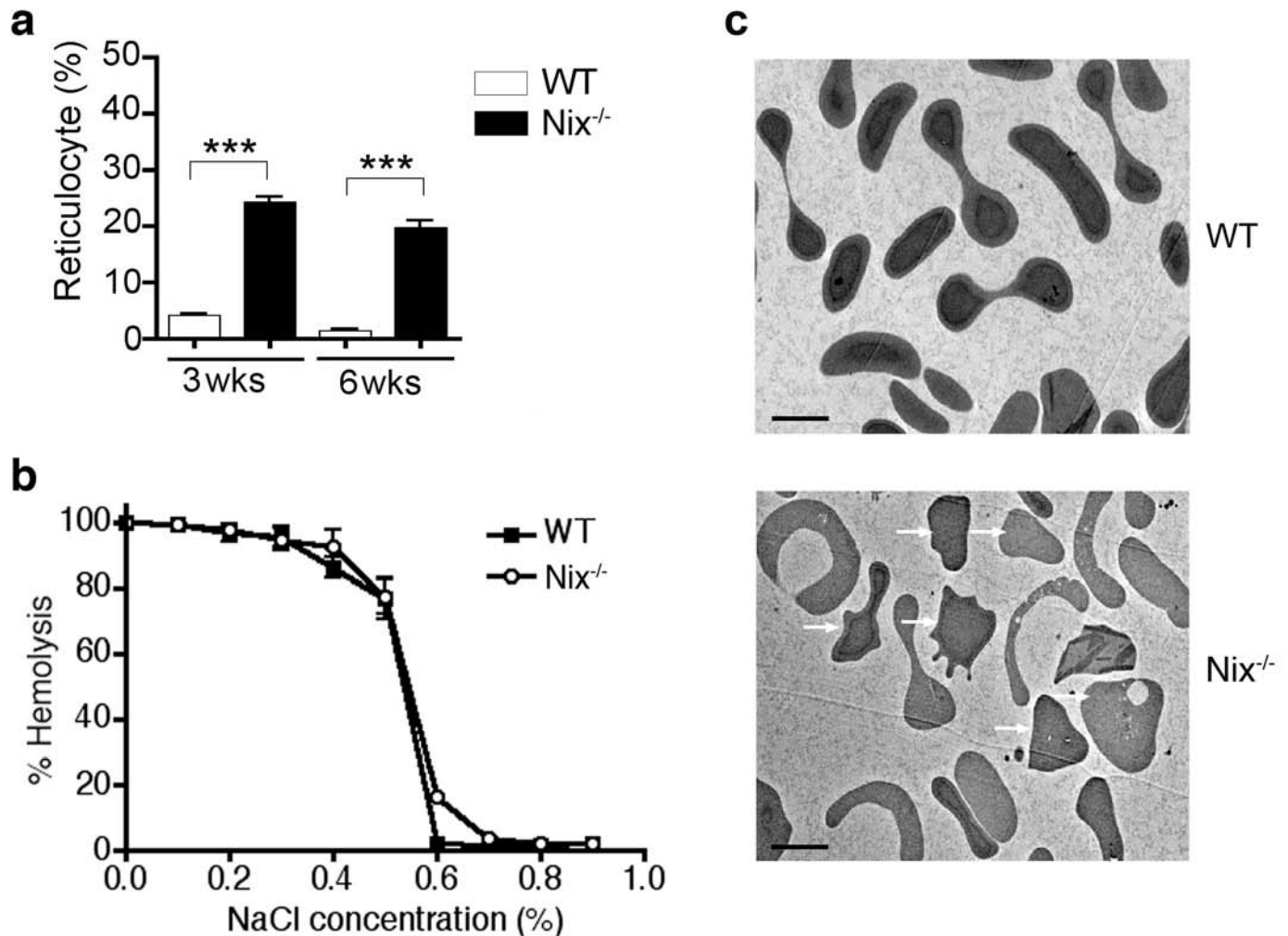
Hematological analyses of wild type (WT) and Nix^{-/-} mice (7 to 12 weeks old) was performed using a Bayer Advia 120 hematology analyzer. WBC, white blood cells; RBC, red blood cells; HB, hemoglobin; HCT, hematocrit; MCV, mean corpuscular volume. Data are presented as mean±s.e.m. and the statistical significance was analyzed by Student's two-tailed *t* test.

Wild type***Nix*^{-/-}**

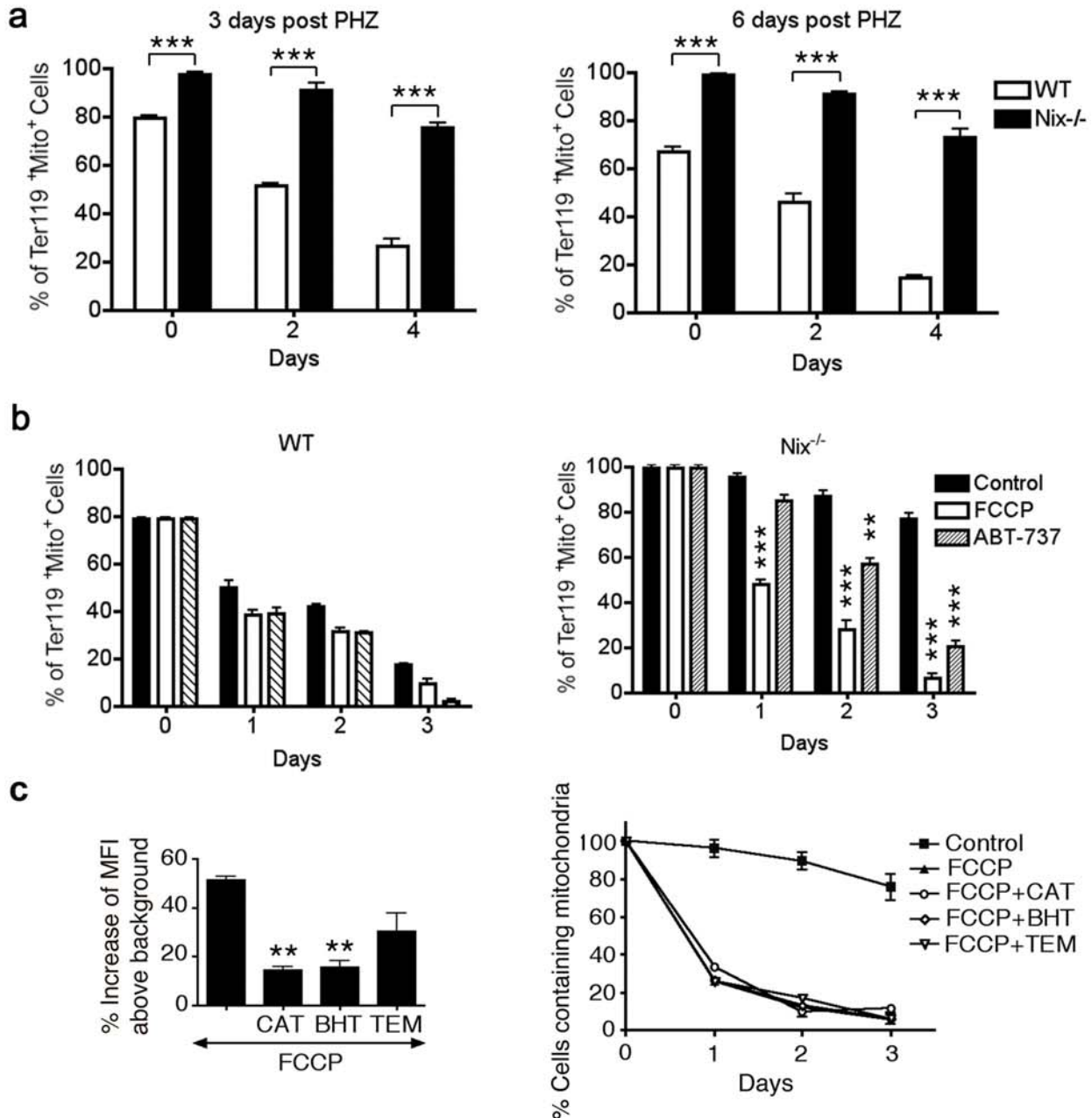
Supplementary Figure 1. A model for Nix in promoting autophagy of mitochondria during erythroid maturation. In wild type RBCs, a maturation signal may lead to the activation of Nix. Nix then induces signaling into mitochondria to trigger the loss of $\Delta\Psi_m$. Mitochondrial depolarization may lead to the changes in the display of lipids and proteins on the outer membrane of mitochondria, facilitating the interactions with autophagosomal membranes and sequestration by autophagosomes. In *Nix*^{-/-} RBCs, the Nix-dependent loss of $\Delta\Psi_m$ is absent. Mitochondria fail to enter the autophagosomes. The uncleared mitochondria are subject to disruption induced by oxidative stress, leading to caspase activation, display of phosphatidylserine and accelerated clearance of RBCs by macrophages.



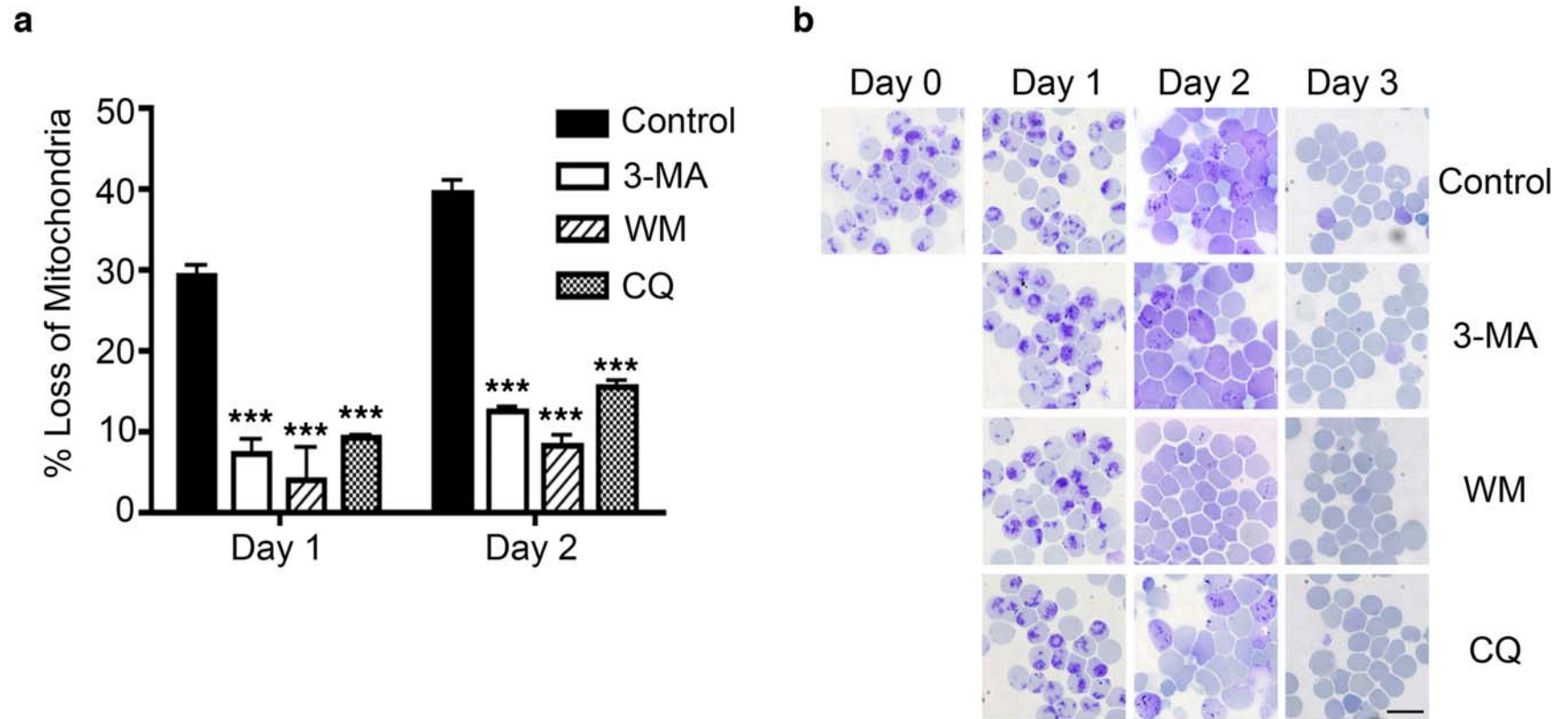
Supplementary Figure 2. Generation of *Nix*^{-/-} mice. **a**, Retroviral insertion of a splice acceptor site (SA), β -geo (lac Z and neomycin), and poly A (pA) between exon 3 and 4 of the *Nix* gene in ES cells. Exon 4 to exon 6 encoding the putative BH3 and mitochondrial transmembrane domain of *Nix* was deleted. *Nix*^{-/-} mice were genotyped using the primers F1 within the gene trap construct, 5'-CTGGATGATCCTCCAGCGCGGGGATC-3'; F2 upstream of the insertion site, 5'-CTGAAGACAGTGACAGTGTACTCAC-3'; and R1 downstream of the insertion site, 5'-CCTTATCTAGTTCTGCTGAAGTTGGC-3'. **b**, Western blot analysis of *Nix* protein in cell lysates from E14.5 Fetal Liver (FL), splenic erythroid cells (ECs) and splenic white blood cells (WBCs) from wild type (+/+) and *Nix*^{-/-} mice. **c**, RT-PCR of *Nix* coding region from WT and *Nix*^{-/-} kidney mRNA using the following primers: *Nix*F: 5'-GTCTCCAGACCATGTCTCACTTAG-3'; *Nix*R: 5'-CGTCTCCCTCAGTAGGTGCTG-3'.



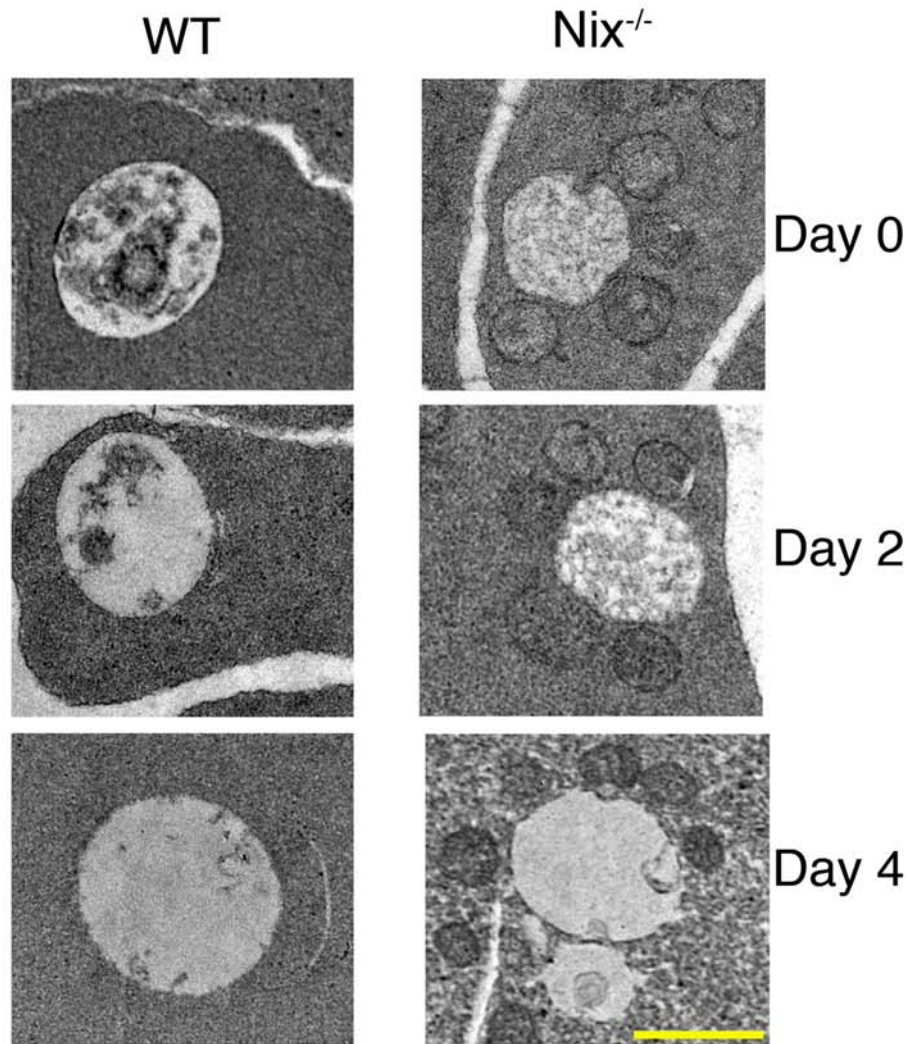
Supplementary Figure 3. Reticulocytosis and osmotic fragility of RBCs in *Nix*^{-/-} mice. **a**, The percentages of reticulocytes measured by brilliant cresyl blue staining (mean±s.e.m.) in the peripheral blood of age-matched wild type (WT) and *Nix*^{-/-} mice ($n=3$ per genotype at each age). *** $P<0.001$. **b**, The osmotic fragility was measured as described (Viscor *et al.*, 1982, *Lab. Anim.* 16: 48-50). Briefly, RBCs (25 μ l) from wild type and *Nix*^{-/-} mice were incubated for 1 h at 37°C in different concentrations of NaCl. The absorbance of the supernatant was measured at 540 nm in a spectrophotometer and absorbance after lysis in water was considered 100%. Results are presented as the mean±s.d. ($n=3$). **c**, RBCs from 6-week-old WT and *Nix*^{-/-} mice were analyzed by transmission electron microscopy. Arrows denote irregular shaped reticulocytes. Scale bar represents 2 μ m.



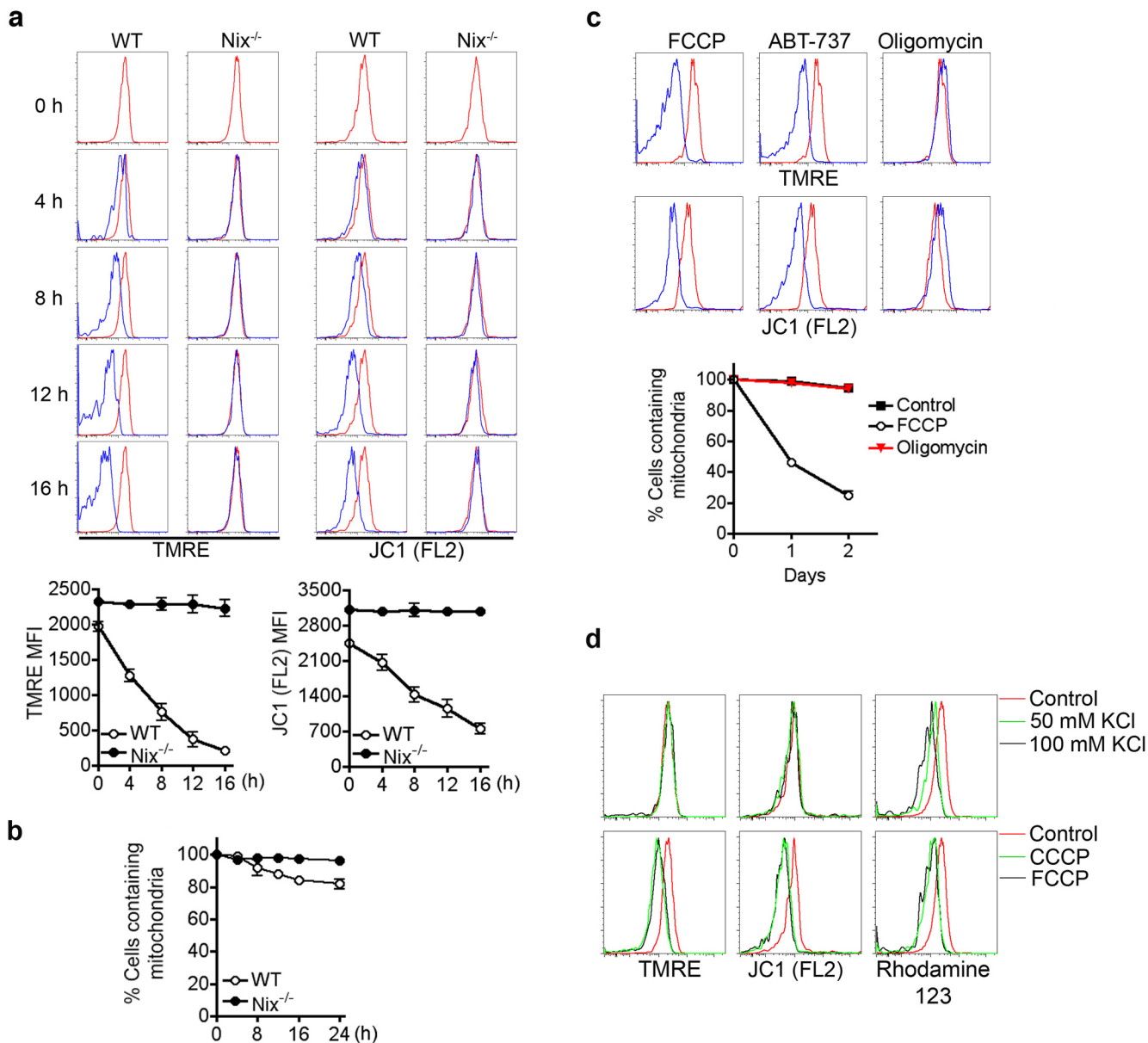
Supplementary Figure 4. Mitochondrial loss in FCCP or ABT-737 treated *Nix*^{-/-} reticulocytes. **a**, Ter119⁺CD71⁺ reticulocytes were sorted from the peripheral blood of WT and *Nix*^{-/-} mice at day 3 or 6 after PHZ treatment. The cells were cultured for *in vitro* maturation for various days, followed by staining with Mitotracker deep red and PE-anti-Ter119. The percentages of Ter119⁺Mitotracker⁺ cells (mean±s.d., *n*=3) after various days of *in vitro* culture were plotted. **b**, Ter119⁺CD71⁺ cells sorted after 6 days of PHZ treatment were cultured with 10 μM FCCP or 1 μM ABT-737, followed by staining as in (a). **c**, FCCP-treated *Nix*^{-/-} reticulocytes were cultured for 2 h in the presence of 4000 U/ml catalase (CAT, Sigma), 100 μM butylated hydroxytoluene (BHT, Sigma), 5 μM tempol (TEM, Sigma) or solvent control (DMSO), and ROS was measured by DCFH-DA staining. The cells were further cultured for 0, 1, 2 and 3 days *in vitro* and cells were stained with Mitotracker deep red. The percentages of mitochondrion containing cells are plotted as the mean±s.d., *n*=3. **P*<0.05, ***P*<0.01, ****P*<0.001



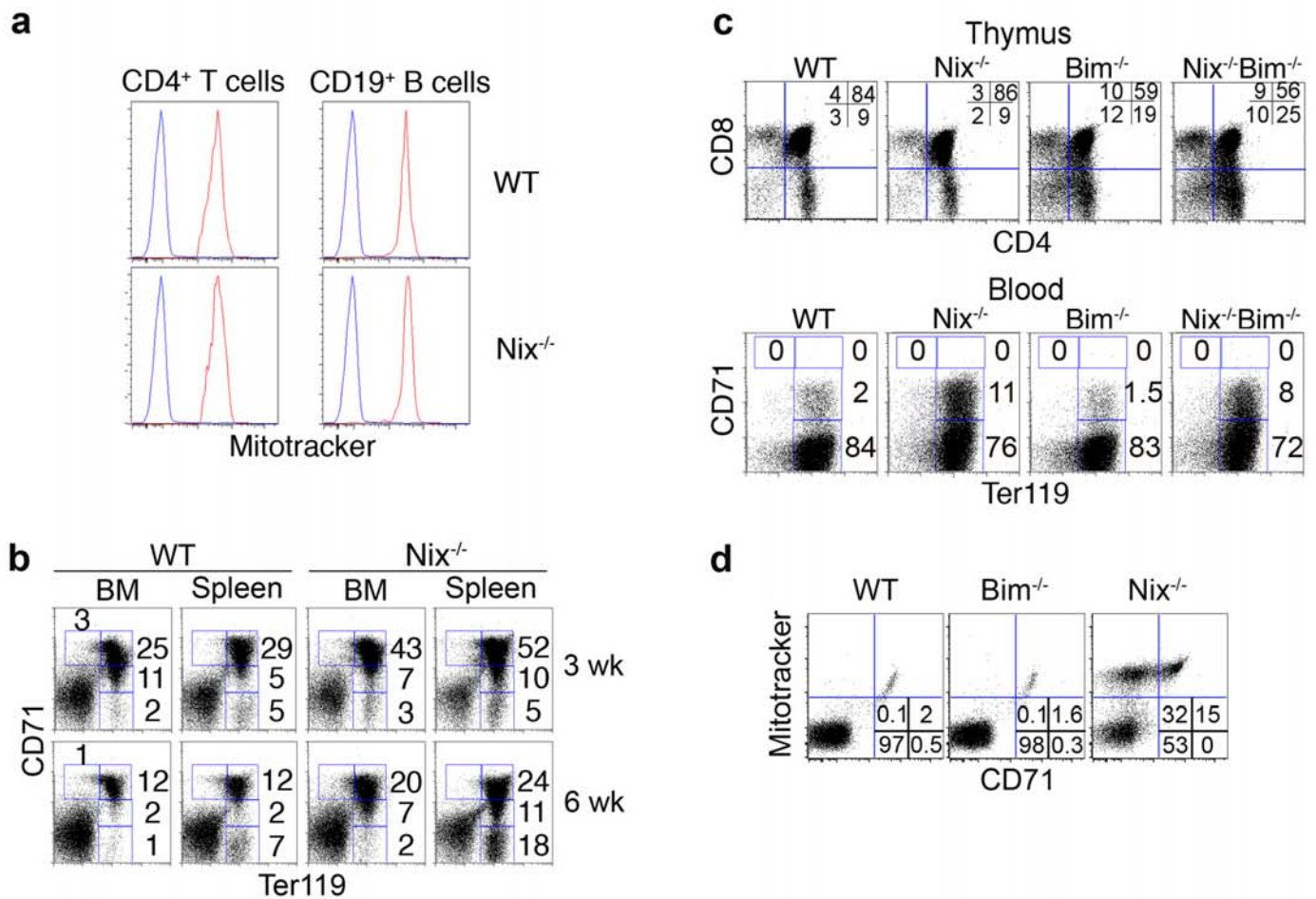
Supplementary Figure 5. Inhibition of autophagy suppresses the removal of mitochondria but not ribosomes in reticulocytes. **a**, WT reticulocytes harvested at day 3 after treatment with PHZ were incubated with 5 mM 3-methyladenine (3-MA), 100 nM wortmannin (WM) or 10 μ M chloroquine (CQ) and cultured for *in vitro* maturation for 1 or 2 days. Cells were stained with Mitotracker deep red and PE-anti-Ter119. The percentages of the loss of mitochondria (mean \pm s.e.m., $n=3$) were plotted. *** $P<0.001$. **b**, The cells as in (a) were cultured *in vitro* for 1, 2, or 3 days. Reticulocytes were stained with new methylene blue. The scale bar represents 20 μ m.



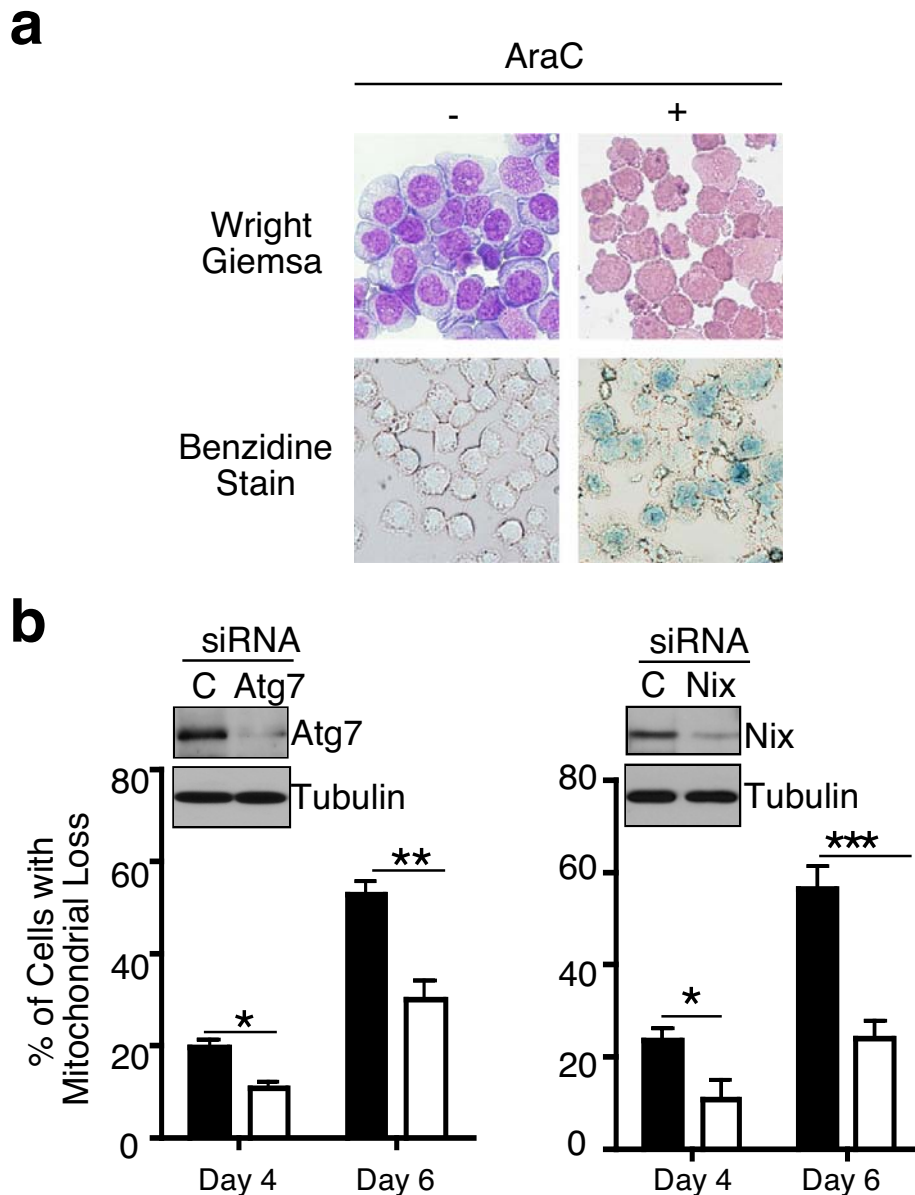
Supplementary Figure 6. Time course of WT and Nix^{-/-} reticulocytes undergoing erythroid maturation. a. WT and Nix^{-/-} reticulocytes harvested at day 3 post-PHZ injections were cultured for *in vitro* maturation for 0, 2 and 4 days. Cells were then analyzed by transmission electron microscopy. Scale bar represents 0.5 μ m.



Supplementary Figure 7. Defects in the loss of $\Delta\Psi_m$ in *Nix*^{-/-} reticulocytes. **a**, WT and *Nix*^{-/-} reticulocytes were cultured *in vitro* for 0 to 16 h, followed by staining with 50 nM tetramethylrhodamine ethyl ester (TMRE) or 10 $\mu\text{g/ml}$ JC1 and analyzed by flow cytometry (red line: 0 h control; blue line: cultured samples). The mean fluorescence intensity (MFI) of TMRE or JC1 (FL2, red) staining (mean \pm s.e.m., $n=3$) was plotted. **b**, WT and *Nix*^{-/-} reticulocytes were cultured *in vitro* for 0 to 24 h. The cells were stained with Mitotracker deep red and analyzed by flow cytometry. The percentages of cells containing mitochondria (mean \pm s.e.m., $n=3$) were plotted. **c**, *Nix*^{-/-} reticulocytes were incubated with (blue line) or without (red line) 10 μM FCCP, 1 μM ABT-737 or 10 $\mu\text{g/ml}$ of oligomycin for 12h (upper panels). Cells were stained with TMRE or JC1 and analyzed by flow cytometry. Incubation with oligomycin which suppresses ATP production by inhibiting F_0F_1 -ATPase resulted in slightly increased $\Delta\Psi_m$ similar to previous observations (Rego *et al.*, *Cell Death Differ.* 8:995-1003, 2001). *Nix*^{-/-} reticulocytes were cultured for *in vitro* maturation with 10 $\mu\text{g/ml}$ oligomycin, 10 μM FCCP or DMSO as solvent control for 0, 1 or 2 days. The percentage of cells containing mitochondria were determined as in (b). **d**, *Nix*^{-/-} reticulocytes were incubated with KCl for 10 min to induce the loss of plasma membrane potential ($\Delta\Psi_p$) (Bortner *et al.*, 1999, *J. Biol. Chem.* 274: 21953-21962), or with 20 μM of cyanide *m*-chlorophenylhydrazine (CCCP) or FCCP for 10 min to disrupt $\Delta\Psi_m$. The cells were stained with 50 nM TMRE, 10 $\mu\text{g/ml}$ JC1 or 10 $\mu\text{g/ml}$ Rhodamine 123 and analyzed by flow cytometry. Rhodamine 123 detected the changes in both $\Delta\Psi_m$ and $\Delta\Psi_p$, while TMRE and JC1 detected changes in $\Delta\Psi_m$ only.



Supplementary Figure 8. Bim and Nix affect lymphoid and erythroid compartments, respectively. **a**, T and B cells from the lymph nodes of wild type (WT) and Nix^{-/-} mice were stained with FITC-anti CD4, PE-anti-CD19 and Mitotracker deep red (Molecular Probes). CD4⁺ or CD19⁺ cells were gated and Mitotracker staining was plotted (blue line: unstained control; red line: Mitotracker staining). **b**, Flow cytometry analysis of erythroid cells from the bone marrow (BM) and spleens of wild type (WT) and Nix^{-/-} mice. Data are representative of three independent experiments. **c**, Nix^{-/-} mice were crossed with Bim^{-/-} mice (The Jackson Laboratory) to obtain Nix^{-/-}Bim^{-/-} mice. Flow cytometry analysis of thymocytes or peripheral blood cells from WT, Nix^{-/-}, Bim^{-/-}, and Nix^{-/-}Bim^{-/-} mice (7-week-old) were performed. Thymocytes were stained with FITC-anti-CD4 and PE-anti-CD8. Peripheral blood cells were stained with FITC-anti-CD71 and PE-anti-Ter119. Data are representative of three independent experiments. **d**, RBCs from WT, Bim^{-/-} and Nix^{-/-} mice (9-week-old) were stained with FITC-anti-CD71, PE-anti-Ter119 and Mitotracker deep red and analyzed by flow cytometry. Ter119⁺ cells were gated and CD71 versus Mitotracker staining was plotted. Data are representative of two independent experiments.



Supplementary Figure 9. The loss of mitochondria in K562 cells undergoing erythroid maturation. **a**, K562 cells were cultured with or without 250 μ M of arabinofuranosylcytosine (AraC, Sigma) for 4 days, followed by staining with Wright-Giemsa (for nuclear staining) or benzidine (for hemoglobin staining) as described (Luisi-DeLuca *et al.*, 1984, *J. Clin. Invest.*, 74: 821-827). **b**, K562 cells were transfected with 2 μ M smartpool siRNA for ATG 7 (filled bars, left panels), Nix (filled bars, right panels) or scrambled siRNA (open bars) as control (C) from Dharmacon by nucleofection (Amaxa). After culture for 48 h, the cells were used for Western blot by probing with antibodies to Atg7 (Cell signaling) or Nix (Kamiya), or treated with 250 μ M AraC for various days. The cells were stained with Mitotracker deep red and analyzed by flow cytometry to determine mitochondrial loss (mean \pm s.d.). * P <0.05; ** P <0.01; *** P < 0.001.